[1]Tongli Chang
[2]Binqi Meng *

Numerical Simulation of Turbine Guide Measurement by Flow Method

Abstract: - In order to solve the vortex band problem in the equipment measuring the exhaust area of the turbine guide by the water flow method, the CFD calculation method was used to analyze the flow velocity, pressure, vorticity distribution characteristic values, flow velocity distribution uniformity and velocity-weighted average angle of the equipment without diversion device and the equipment with diversion device. The results show that when the diversion device is not set, there are large-scale surface vortices and sub-surface vortices in the water tank, large-scale backflow above the turbine guide, and there are high-speed and high-vorticity regions in the turbine blades, which leads to the deterioration of the flow regime in the equipment, which has a great impact on the measurement accuracy. After setting up the diversion device, it was found that the uniformity of the flow velocity in the section in the equipment changed significantly, the flow field became more uniform, the characteristic values of the vorticity distribution of the measured section decreased, and the characteristic values of the vorticity distribution on the longitudinal profile of the axis above the turbine guide decreased from 0.672 to 0.403. The evenness of flow velocity distribution and the weighted average angle of velocity in each section were improved, which were increased by 4.3%~5.2% and 1.4%~1.6%.

Keywords: Water flow method; Turbine guide; Diversion device; Numerical simulation; Vortex

0 INTRODUCTION

There are various methods to measure the exhaust area of turbine nozzles, including water flow measurement [1], mechanical gauges [2], and coordinate measuring machine (CMM) [3]. This paper focuses on the study of the water flow method. The water flow test equipment is used to detect the flow capacity of high-pressure turbine nozzles. The internal flow pattern and hydraulic characteristics have a significant impact on measurement accuracy. Therefore, during the design of the equipment, it is crucial to ensure its stability and uniform flow velocity [4]. Improper design of the equipment can lead to undesirable flow patterns, which are mainly manifested in two ways: firstly, large-scale surface vortices on the water surface can directly affect the accuracy of the measurement; secondly, vortices at the inlet and inside the turbine nozzle can introduce air into the chamber when intermittent suction vortices or through-flow suction vortices occur at the outlet and inside, causing equipment vibration and affecting operational safety [5]. Depending on their location, vortices can be classified into two categories: free-surface vortices and subsurface vortices [6]. The emergence of each type of vortex can bring about numerous hazards and impacts. On the one hand, it enhances water turbulence, deteriorates flow conditions, and forms a two-phase flow of water and air or an alternating flow of the pressure section [7]; on the other hand, it reduces the flow area and increases the flow resistance, resulting in decreased flow rate [8]. Furthermore, the two-phase flow of water and air generated by vortices can cause water pulsation,

[1] * School of Mechanical and Electrical Engineering, Northeast Forestry University Harbin 150040, Heilongjiang, China.
[2]School of Mechanical and Electrical Engineering, Northeast Forestry University Harbin 150040, Heilongjiang, China.Email:13124517693@163.com

and the resulting additional pressure can impose additional loads on the device walls. These vortices should be avoided as much as possible [9]. However, due to the unique structure of turbine nozzles, when water flows through the narrow throat area of the turbine nozzle, ideal hydraulic conditions cannot be achieved within the device, instead, large-scale recirculation suction vortices and other phenomena occur. Therefore, it is necessary to design reasonable vortex elimination and prevention measures.

Many scholars have conducted numerical simulations to study the formation of vortices. For example, Ye Mao [10], Chen Yunliang [11], and Constantinescu [12] used the Reynolds-averaged Navier-Stokes (RANS) equations and $k-\varepsilon$ turbulence models to study vertical axis vortices through experiments and numerical simulations. Based on literature research, while there are not many studies on water flow experimental devices, there are numerous cases of vortex elimination research both domestically and internationally. The impact of vortices can be reduced by optimizing device design, improving operational methods, and installing vortex elimination devices. Liu Chao [13] et al. conducted vortex elimination experiments on water flow channels and found that the use of zigzag vortex elimination strips can effectively eliminate vortices and significantly enhance hydraulic characteristics. Similarly, Wang Yajun [14] proposed the installation of triangular guide piers for flow rectification to reduce the impact of vortices.

Drawing on previous studies on various rectification measures, this paper focuses on water flow experimental devices and utilizes numerical simulations to analyze the influence of flow guide devices on the flow patterns within these devices. The goal is to provide a reference for the design of equipment used in the water flow method to measure the throat area of turbine nozzles.

1 RESEARCH OBJECT

The cross-sectional diagram of the exhaust area of the measured turbine nozzle is shown in Figure 1. The overall structure diagram of the water flow test equipment is presented in Figure 2, with specific parameters detailed below: The height of the water tank is 5000mm, with a radius of 1500mm for the upper half and a radius of 400mm for the lower half. The water surface area of the tank is at least 20 times the exhaust area of the measured nozzle. The inner ring of the measured nozzle has a radius of 270mm and a thickness of 8mm. The outer ring has a radius of 360mm with a minimum thickness of 2mm. The base plate of the central through-hole has a radius of 365mm and a thickness of 10mm. The support has a radius of 380mm and a thickness of 5mm. The pressing plate has a radius of 400mm and a thickness of 5mm. The baffle, which prevents fluid from flowing out of the central through-hole of the turbine nozzle, has a radius of 270mm and a thickness of 5mm.

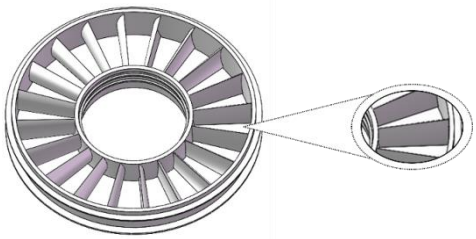

Fig.1 Structural model of a turbine director

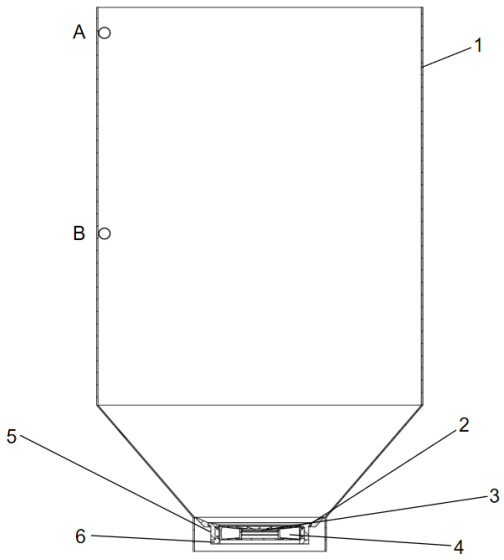

1.Water Tank 2.Pressing Plate 3.Deflector 4.Nozzle Guide Vane 5.Support 6.Base Plate

Fig.2 The overall structure of the traditional water flow experimental device

During the test, first fill the tank with water and allow it to stand for a period to settle. Drain the water and start the timer when the water level reaches point A. Stop the timer when the water level drops to point B. Record the time required for the water surface to pass between the two measurement points. By comparing this time with the time required for water to flow through a known area standard part under the same conditions, the throat area of the turbine nozzle guide vane can be calculated [1]. The calculation formula is as follows:

$$A_1 = \frac{A_2 T_2}{T_1} \tag{1}$$

A1 represents the throat area of the nozzle guide vane to be measured, A2 represents the calibrated area of the standard part, T2 represents the time required for water to flow through the standard part, and T1 represents the measured time for water to flow through the nozzle guide vane being tested.

2 NUMERICAL SIMULATION

2.1 Governing Equations

The flow within the box belongs to incompressible turbulent flow, and the Reynolds-averaged Navier-Stokes (RANS) method is adopted for its turbulent numerical calculation. In the main flow region of the box, the flow is generally in a high Reynolds number turbulent state, and since the fluid needs to pass through the narrow turbine guide vane throat at high speed, there is often a large-scale backflow in the box. Therefore, the RNG $k-\varepsilon$ model among the two-equation $k-\varepsilon$ models is used for solving [15].

Kinetic Energy Equation (K Equation):

$$\frac{\partial(\rho k)}{\partial t} + \frac{\partial}{\partial x_i}(\rho u_i k) = \frac{\partial}{\partial x_j}\left[\alpha_k \mu_{eff} \frac{\partial k}{\partial x_j}\right] + G - \rho\varepsilon \tag{2}$$

Dissipation Equation (ε Equation):

$$\frac{\partial(\rho\varepsilon)}{\partial t}+\frac{\partial(\rho u_i k)}{\partial x_i}=\frac{\partial}{\partial x_j}\left[\alpha_\varepsilon \mu_{eff}\frac{\partial \varepsilon}{\partial x_j}\right]+C_{1\varepsilon}^{*}\frac{\varepsilon}{k}G-C_{2\varepsilon}\rho\frac{\varepsilon^2}{k} \tag{3}$$

2.2 Boundary Conditions and Mesh Generation

In the numerical simulation, the professional modeling software SOLIDWORKS was used to geometrica lly model the water flow experimental device. Structured "O-grid" body-fitted meshes were generated u sing ICEM, and the surfaces of more complex flow components such as blades were refined. To simpl ify the boundary conditions and influencing factors under study and improve mesh quality, the model was simplified during modeling by omitting parts such as the base plate and supports. The total numbe r of meshes was 689,123, with 126,556 mesh nodes. The maximum size of the global element was 0.1 m, and the refined size in some areas was 0.05m. The mesh of the computational domain is shown in Figure 3. The pressure-based transient solver was selected as the solution method, with the gravity dir ection of the mesh set. The Volume of Fluid (VOF) method was used to solve the free surface flow. The implicit parametric equation was chosen, and the SIMPLEC algorithm was utilized for coupled cal culations. To improve calculation accuracy, the volume fraction and other terms were set to a second-or der upwind scheme. The inlet boundary of the box was set as a pressure inlet, while the outlet of the box employed a free outflow boundary condition. Standard wall functions were applied to all wall sur faces.

Fig.3 Compute domain grid for water flow experiment equipment

3 RESULTS ANALYSIS

3.1 Improved Design Scheme of Vortex Elimination Device

During the operation of the traditional water flow experimental device in this experiment, large vortices would appear, affecting the time accuracy of reading points A and B. Moreover, when the water flow entered the turbine guide vane, vortices occurred in the middle of the guide vane, resulting in uneven loading on the guide vane, which subsequently imposed significant impacts on the turbine guide vane blades, shortening their service life. Therefore, this paper designed a cylindrical flow guide plate and a hemispherical flow guide plate. The conical section above the cylindrical flow guide plate can effectively divert the water body to the bottom of the box, while the outer surface of the hemispherical flow guide plate remains parallel to the conical section of the box. This arrangement can improve the flow pattern of the water body before it passes through the turbine, enabling a smooth transition of the water body to the turbine guide vane under test. The cylindrical flow guide plate was installed below point B, while the hemispherical flow guide plate replaced the original baffle. The specific structural diagram is shown in Figure 4.

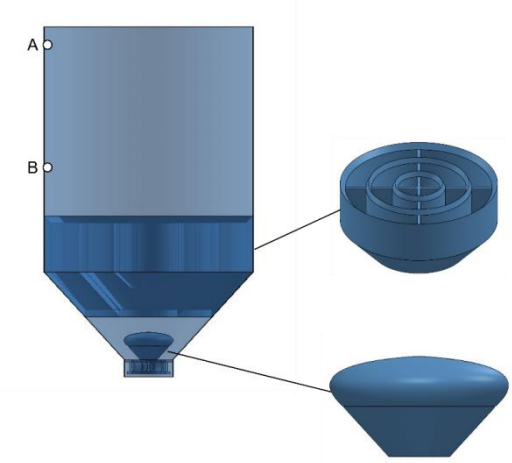

(a) Schematic Diagram of the Overall Structure

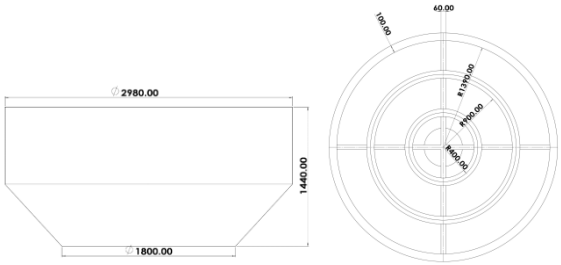

(b) Schematic Diagram of the Dimensions of the Cylindrical Deflector Plate

Fig.4 Schematic diagram of the structure (in mm)

3.2 Comparative Analysis of Flow Patterns After Improvement

3.2.1 Comparative Analysis of Horizontal Cross-Sectional Flow Patterns at Points A and B

This paper conducts a comparative analysis of the velocity contour plots (Figures 5 and 7) and vorticity contour plots (Figures 6 and 8) at cross-sections A and B, with and without the flow guide device (for the sake of clarity, the following figures (a) represent the design scheme without the flow guide device, and figures (b) represent the design scheme with the flow guide device).

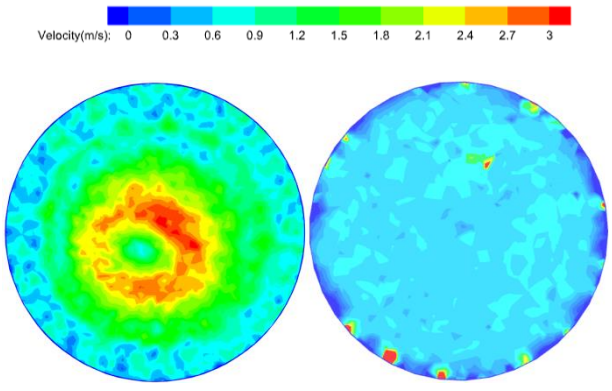

（a） （b）

Fig.5 Comparison of velocity contours of point A slices

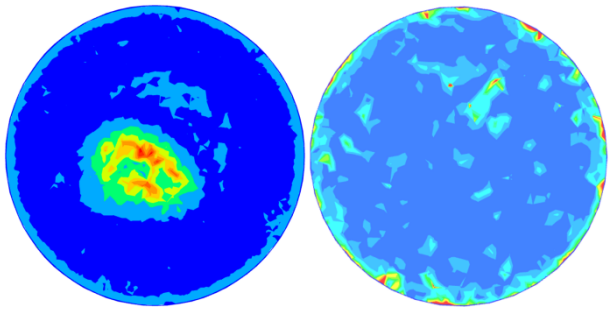

（a） （b）

Fig.6 Comparison of vorticity contours of point A slices

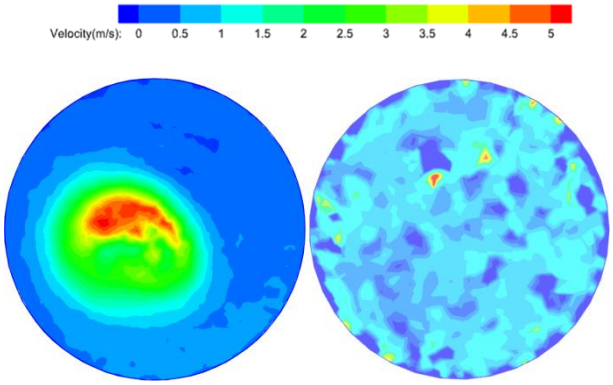

（a） （b）

Fig.7 Comparison of velocity contours of point B slices

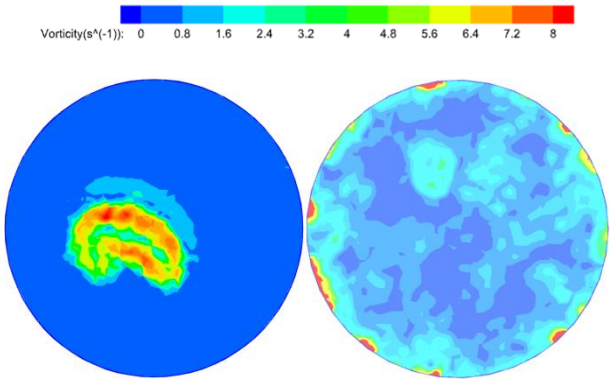

（a） （b）

Fig.8 Comparison of vorticity maps of point B sections

Obviously, experimental observations revealed that vortices inevitably arise due to the high flow velocity through the conical section and the flow bypass effect of the water body flowing through the turbine guide vane. This phenomenon is most pronounced in devices without flow guide plates. By comparing the velocity contour plots and vorticity contour plots, it can be seen that larger vortices appear in the middle region of the original device, with highly uneven velocity distribution. Specifically, the minimum velocity at cross-section A is 0.1m/s, and the maximum velocity is 2.8m/s, while at cross-section B, the minimum and maximum velocities are 0.3m/s and 5.1m/s, respectively. This significantly impacts measurement accuracy, and the impact of vortices on the inner wall also reduces the service life of the equipment. In contrast, the flow guide plates in the device with flow guide devices can improve the flow pattern, enabling a smoother transition of the water body to the conical section of the box and a more uniform velocity distribution. Most areas of cross-section A have velocities ranging from 0.3m/s to 1m/s, while most areas of cross-section B have velocities ranging from 0.2m/s to 2.3m/s. Furthermore, comparing the vorticity contour plots shows that the maximum vorticity values at cross-sections A and B of the original device are 5.4s-1 and 8.2s-1, respectively, while those of the improved device are 4.7s-1

and 7.4s-1, respectively. This indicates that the flow guide devices can effectively divert the flow, disrupt the formation of vortices, and significantly reduce their occurrence, enabling more accurate measurements of the time taken for the water flow to pass through cross-sections A and B of the device.
Additionally, Zi Dan [16] proposed a new quantitative index Ω for evaluating the vorticity field when studying the optimization methods of pump station intake basins. The formula is:

$$\Omega = \varpi_{\mathrm{P}} \left(\varpi_{\max} - \varpi_{\min} \right) R^6 / Q^2 \tag{4}$$

$$\varpi_{\mathrm{P}} = \frac{1}{n} \sum \sqrt{\varpi_j^2} \tag{5}$$

In the formula: Ω represents the characteristic of vorticity distribution in the cross-section; ϖ_{P} is the average value of the partial vorticity; $\varpi_{\max}$ is the maximum value of the partial vorticity; $\varpi_{\min}$ is the minimum value of the partial vorticity; R is the radius; Q is the flow rate; n is the number of cross-sectional units; and ϖ_j is the partial vorticity of each unit j.
The Ω values for cross-section A shown in Figure 6 are 0.433 and 0.296, respectively. The Ω values for cross-section B shown in Figure 8 are 0.523 and 0.317, respectively. A smaller Ω value indicates a smoother water flow. In summary, the flow guide device can make the flow pattern more stable and improve the uniformity of velocity distribution.

3.2.2 Comparative Analysis of Flow Patterns of Turbine Guide Vanes

The velocity contour plots, vorticity contour plots, and pressure contour plots of the original design scheme and the design scheme with flow guide devices are shown in Figures 9-11, respectively.

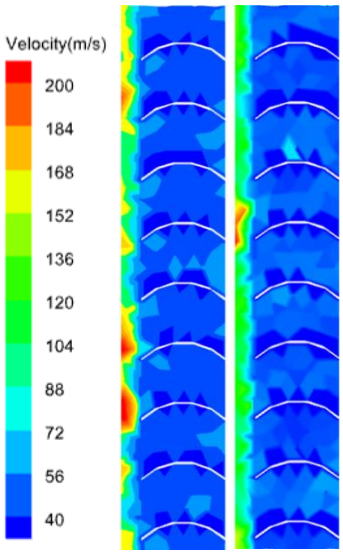

（a） （b）

Fig.9 Comparison of impeller airfoil unfolded diagram (velocity contour diagram)

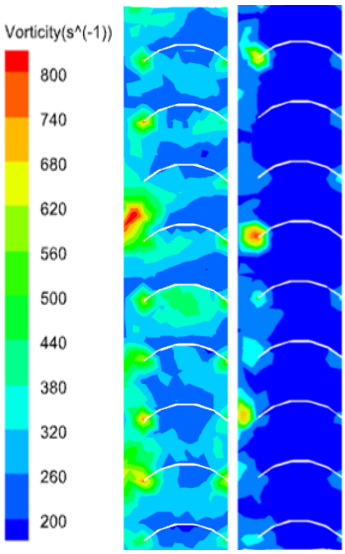

（a） （b）

Fig.10 Comparison of impeller airfoil unfolded diagram (vorticity contour diagram)

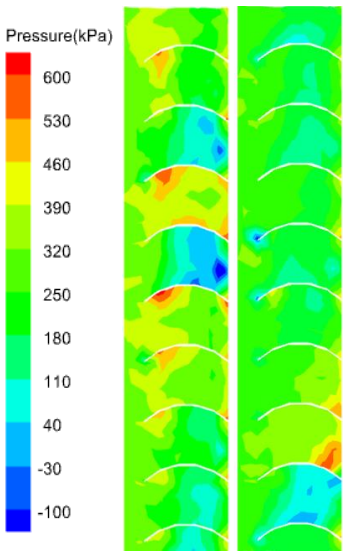

（a） （b）

Fig.11 Comparison of impeller airfoil unfolded diagram (pressure contour diagram)

When water flows through the turbine guide vane, the narrow exhaust area of the vane causes a sudden increase in velocity, which can easily lead to equipment vibration, deteriorate the flow pattern, and affect measurement accuracy. As seen from the velocity contour plots, vorticity contour plots, and pressure contour plots, the internal water velocity, vorticity, and pressure distribution of the guide vane with a hemispherical flow guide plate are more uniform. The outer wall of the hemispherical flow guide plate is parallel to the conical section of the box, allowing the water to disperse the incoming flow before entering the turbine guide vane and reorganize the water to enter the throat of the guide vane more smoothly, ensuring the uniformity of the water and allowing it to enter the turbine guide vane more steadily. Ordinary baffles can only prevent water from entering the central through-hole of the turbine, but they cannot effectively disperse the incoming flow, resulting in a large number of vortices in the middle of the turbine blades. This uneven load on the blades leads to uneven static pressure distribution in the guide vane area, affecting measurement accuracy and, in severe cases, damaging the turbine guide vane structure.

Figures 12 and 13 compare the vorticity contour plots and velocity contour plots of the axial cross-section of the turbine guide vane, respectively. It can be seen that the area occupied by vortices in the device with ordinary flow guide plates is larger, with intense vortex motion and chaotic flow patterns within the flow field. In contrast, the state presented by the spherical flow guide plate is the opposite. Additionally, by calculating the quantitative

index Ω for evaluating the vorticity field mentioned earlier, the values are 0.672 and 0.403, respectively. The vortex intensity in Scheme b is weaker, indicating better flow patterns.

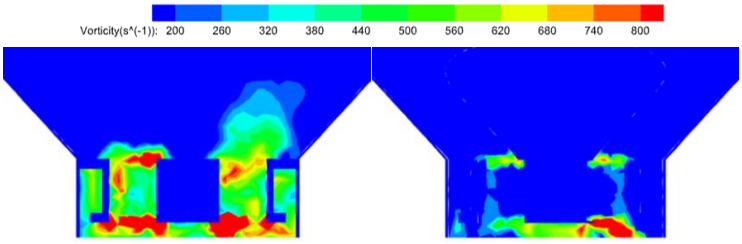

（a） （b）

Fig.12 Comparison of axis slice plots (vorticity contour diagram)

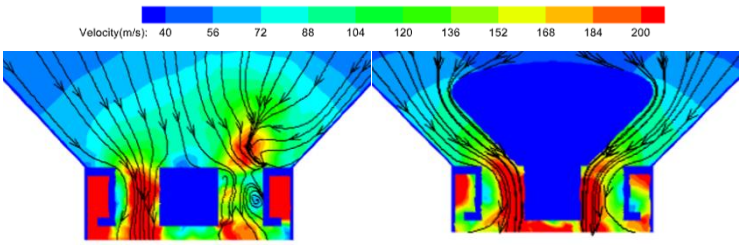

（a） （b）

Fig.13 Comparison of axis slice plots (velocity contour diagram)

3.2.3 Analysis of Velocity Uniformity

In fluid equipment, it is almost impossible to achieve a perfectly ideal flow field, but it is feasible and necessary to bring it to the best possible condition. To evaluate the quality of the inlet conditions, the uniformity V_u of the axial velocity distribution across the cross-section and the weighted average angle θ of the velocity distribution are introduced. The closer V_u is to 100%, the more uniform the axial velocity distribution across the cross-section is; the closer θ is to 90°, the closer the water flow across the cross-section is to being perpendicular to the horizontal cross-section, indicating more ideal inlet conditions [17]. The calculation formulas are as follows:

$$V_u = \left[1 - \frac{1}{\overline{u_a}} \sqrt{\frac{\sum \left(u_{ai} - \overline{u_a}\right)^2}{m}}\right] \times 100\% \tag{6}$$

$$\theta = \sum u_{ai} (90^\circ - \arctan \frac{u_{ti}}{u_{ai}}) / \sum u_{ai} \tag{7}$$

Where: V_u is the uniformity of velocity distribution; θ is the average angle of velocity distribution; m is the number of units in cross-section i; $\overline{u_a}$ is the average axial velocity of the cross-section; u_{ai} is the axial velocity of each unit in cross-section i; u_{ti} is the transverse velocity of each unit in the cross-section.

Taking the horizontal cross-sections of chambers A and B, as well as the height above the turbine guide vane plane as the analysis objects, Figure 14 shows that the velocity distribution uniformity across the horizontal cross-section above the turbine guide vane is significantly improved with the flow guide device compared to without it, with an average improvement of approximately 5%. According to Table 1, the velocity distribution uniformity and the velocity deviation angle of cross-section A increase by 5.2% and 1.6° respectively compared to the original scheme, while those of cross-section B increase by 4.3% and 1.4° respectively. The above indicates that the equipment with flow guide devices can effectively improve the adverse flow patterns near the chambers and turbine guide vane, reduce the generation of harmful vortices, mitigate the vibration caused by water flow, ensure the optimal operating state of the equipment, and enable more accurate readings of the time values of water flowing through each cross-section.

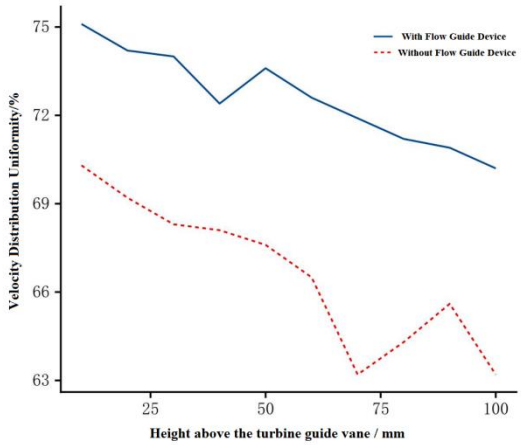

Fig.14 Comparison of the uniformity of the velocity distribution at the height above the turbine guide

Tab.1 Cross-sectional flow regime

Cross-Section	**A**		**B**	
Evaluation Metrics	**Velocity Distribution Uniformity V_u /%**	**Velocity Deviation Angle θ / (°)**	**Velocity Distribution Uniformity V_u /%**	**Velocity Deviation Angle θ / (°)**
Without Flow Guide Device	73.2	80.6	70.3	78.1
With Flow Guide Device	78.4	82.2	74.6	79.5
Increase	5.2	1.6	4.3	1.4

4 CONCLUSION

This paper takes the water flow experimental equipment as the research object and studies the rectification effects of the original scheme and the scheme with flow guide devices on the flow pattern of the equipment from multiple aspects, including the horizontal cross-sections A and B of the tank and the turbine nozzle guide vane blades. The following conclusions can be drawn:

(1) When no flow guide measures are installed inside the equipment, the flow pattern is relatively chaotic, with obvious vortices appearing in the cross-sections A and B as well as in the guide vane area. This is detrimental to accurately reading the time it takes for the water surface to flow through the measured cross-section, affecting the precision of measuring the throat area of the turbine nozzle guide vane.

(2) Based on the CFD method, the water flow conditions during equipment operation were simulated. The results show that after installing flow guide devices, the water flow in cross-sections A and B becomes more uniform, with the vorticity distribution eigenvalues reduced to 0.296 and 0.317, respectively. There are no obvious vortices that could affect measurement accuracy, and the probability of vortices occurring inside the turbine nozzle guide vane is greatly reduced. Additionally, the flow pattern before the water enters the guide vane becomes smoother, and the turbine distribution eigenvalue on the vertical cross-section along the axis above the turbine nozzle guide vane decreases from 0.672 to 0.403, resulting in less impact on the turbine. The uniformity of flow velocity distribution in the horizontal cross-sections A and B with flow guide devices is improved by 5.2% and 4.3%, respectively. The average uniformity of flow velocity distribution in the horizontal cross-section above the turbine nozzle guide vane is improved by approximately 5%.

(3) The use of flow guide devices inside the equipment not only improves the water flow pattern but also makes the vorticity distribution inside the tank more uniform, effectively eliminating large-scale vortices and

enhancing the accuracy of measuring the exhaust area of the turbine nozzle guide vane, meeting the expected operational requirements.

REFERENCE

[1] Zheng T, Zhao K, Wu R. Measurement of turborotor throat area by water flow[J]. Journal of Propulsion Technology,1997, 18(4): 106-108.

[2] Zhu H, Zhou H, Pu L, et al. Direct measurement de-vice for the exhaust area of the throat of the engineturbine director[J]. Automation & Instrumentation,2012,(06):130-132.

[3] Yang Haicheng, Wang Yu, Ding Yiqi. Measurement a-nd analysis of exhaust area of turbine guide[J].Aeronautical Precision Manufacturing Technology,2016,52(03):56-58+62.

[4]Long N I, Shin B R. Study on surface vortices in pump sump [J]. Journal of Fluid Machinery, 2012, 15(5): 60-66.

[5] Tokyay T E, Constantinescu S G. Large eddy simulation and Reynolds averaged Navier-Stokes simulations of flow in a realistic pump intake: a validation study[M]//Impacts of global climate change. 2005: 1-12.

[6] Chan L ,Chin C ,Soria J , et al.Large eddy simulation and Reynolds-averaged Navier-Stokes calculations of supersonic impinging jets at varying nozzle-to-wall distances and impinging angles[J].International Journal of Heat and FluidFlow,2014,4731-41.

[7] Bayeul-Lainé A C, Simonet S, Bois G, et al. Two-phase numerical study of the flow field formed in water pump sump: influence of air entrainment[C]//IOP Conference Series: Earth and Environmental Science. IOP Publishing, 2012, 15(2): 022007.

[8] Samsudin M L, Munisamy K M, Thangaraju S K. Application of multiphase modelling for vortex occurrence in vertical pump intake-a review[C]//IOP Conference Series: Materials Science and Engineering. IOP Publishing, 2015, 88(1): 012024.

[9] Desmukh T S, Gahlot V K. Numerical study of flow behavior in a multiple intake pump sump[J]. International Journal of Advanced Engineering Technology, 2011, 2(2): 118-128.

[10] Ye Mao, Wu Chao, Chen Yunliang, et al. model investigation and numerical simulation of vertical vortex [J].Journal of Hydroelectric Engineering,2007,(01):33-36.)

[11] Chen Y, Wu C, Ye M. Research on flow field characteristics of vertical vortex with multi-circle spiral flow[J]. Journal-Sichuan University Engineering Science Edition, 2007, 39(1): 13-17.

[12]Constantinescu G S, Patel V C. Numerical model for simulation of pump-intake flow and vortices[J]. Journal of Hydraulic Engineering, 1998, 124(2): 123-134.

[13] Chao L, Fan Y, Jun Z. Analysis of the vortex-elimination device of pump suction passage using high-speed photography [J]. Transactions of the Chinese Society for Agricultural Machinery, 2014, 45(3): 61-65.

[14] Wang Yajun. The eddy-prevention methods in the closed sump of pumping station by CFD [D].Yangzhou University,2016.

[15]Cheng L, Liu C, Zhou J, et al. The study on the flow fields and hydraulic performance in the pump sump[C]//Fluids Engineering Division Summer Meeting. 2007, 42894: 831-839.

[16] Zi D, Wang F, Yao Z, et al. Effects analysis on rectifying intake flow field for large scale pumping stati-on with combined diversion piers[J]. Transactions of the Chinese Society of Agricultural Engineering, 2015， 31(16): 71-77.

[17] Lu Linguang, Cao Zhigao, Zhou Jiren. Optimized hydraulic calculations for open inlet basins [J]. Journal of Hydraulic Engineering,1997,(03):17-26

FUNDING

This work was supported by the funding project of Heilongjiang Provincial Industry and Information Technology Commission (GXW2010080) and the funding project of Heilongjiang Provincial Department of Education (11553020).

ABOUT THE AUTHOR

Tongli Chang was born in Harbin，Heilongjiang. China, in 1968. He received his Ph.D. from Harbin Institute of Technology. He is now an associate professor at Northeast Forestry University. His main research direction is hydraulics and bionic robots.

E-mail: tonglichang@126.com

Binqi Meng was born in Harbin， Heilongjiang. China, in 1999. He received his engineering degree from Northeast Forestry University. He is currently pursuing a master's degree at Northeast Forestry University. His main research direction is measurement of the turbine guides.

E-mail: 13124517693@163.com